Magnetic properties of icosahedral Al-Pd-Mn quasicrystals

F. Hippert,[1,*] M. Audier,[1] J. J. Préjean,[2] A. Sulpice,[2] E. Lhotel,[2] V. Simonet,[3] and Y. Calvayrac[4]
[1]*Laboratoire des Matériaux et du Génie Physique, ENSPG, F-38402 Saint Martin d'Hères Cedex, France*
[2]*Centre de Recherches sur les Très Basses Températures, CNRS, BP 166, F-38042 Grenoble Cedex-9, France*
[3]*Laboratoire Louis Néel, CNRS, BP 166, F-38042 Grenoble Cedex-9, France*
[4]*CECM/CNRS, 15 rue G. Urbain, F-94407 Vitry Cedex, France*
(Received 9 April 2003; published 2 October 2003)

The magnetic properties of icosahedral Al-Pd-Mn phases have been investigated by studying a large set of samples, including single crystals and polycrystalline ribbons. The composition and structure (F, F_2, or F_{2M}) of each sample have been determined. Composition changes and thermal treatments lead to a wide range of magnetic susceptibility variations (by a factor around 55). The comparison of susceptibility data for all studied samples, as well as for literature samples, shows that the temperature dependence of the magnetic susceptibility exhibits a universal behavior, whatever the structural state, composition, and thermal treatment. It can be accounted for by a Kondo effect gradually affected by magnetic RKKY-type interactions as the concentration of magnetic Mn atoms increases. The magnetic Mn atom concentration is small, ranging from 3.8×10^{-5} for the less magnetic sample studied up to 2×10^{-3} for the more magnetic one—i.e., much less than the Mn concentration in the icosahredral phase ($\sim8\times10^{-2}$). It varies with thermal treatments and depends strongly on the composition of the icosahedral phase. In particular, the magnetic properties are found to evolve along the growth direction of a large single grain obtained by the Czochralski technique in relation with composition variations.

DOI: 10.1103/PhysRevB.68.134402 PACS number(s): 75.20.Hr, 75.50.Lk, 61.44.Br

I. INTRODUCTION

The magnetic properties of quasicrystalline icosahedral Al-Pd-Mn phases have attracted much attention. The presence of localized moments is revealed by Curie-like terms in the temperature dependence of the magnetic susceptibility.[1–13] In contrast, most Al-based quasicrystals (QC's), such as, for instance, in Al-Cu-Fe,[14] Al-Cu-Co,[15] and Al-Pd-Re systems,[16] exhibit a nearly temperature-independent negative magnetic susceptibility and hence no localized moments.

The Curie terms measured in icosahedral Al-Pd-Mn phases are much smaller than those expected if all Mn atoms have a spin value $S=5/2$. This is due to the fact that most of the Mn atoms are nonmagnetic, as is proved from nuclear magnetic resonance (NMR) studies.[9,17] This behavior is in strong contrast with that of liquids in equilibrium with these phases, where most of the Mn atoms are magnetic.[18]

In view of the small Curie constants measured in icosahedral Al-Pd-Mn phases, it is first necessary to examine whether the Mn atoms which are magnetic are located in the quasicrystalline phase or in foreign phases, undetected in structural studies. The observation of spin-glass transitions at low temperature (a few K or less) in several samples suggests that magnetic Mn atoms are diluted in the QC phase and coupled through indirect Ruderman-Kittel-Kasuya-Yoshida (RKKY) interactions mediated by conduction electrons.[4,5,19–21] Also, in NMR experiments, the broadening of the ^{27}Al resonance line, observed through a temperature decrease, results from magnetic Mn atoms located within the icosahedral phase.[9,17]

The existence of magnetic Mn atoms in the quasicrystalline structure must be related to particular environments. The influence of local and medium range atomic structure on moment formation in Al-Pd-Mn and Al-Mn quasicrystals and approximant phases has been established by theoretical studies.[22–24] These predictions could be confirmed in the case of approximant phases where sites occupied by magnetic Mn atoms could be identified.[25–27] Let us recall that approximants are periodic phases, with large unit cells and structures closely related to that of quasicrystals, which can be described as packings of icosahedral clusters, also considered in quasicrystalline structural models. However, in the case of quasicrystals, the identification of magnetic Mn atoms remains a very difficult task because their atomic concentration never exceeds a few 10^{-3} and even can be as small as 3.8×10^{-5} (as shown hereafter).

Despite a great amount of works devoted to the magnetic properties of Al-Pd-Mn icosahedral phases,[1–13] the parameters determining the magnetic Mn concentration are still far from being completely understood. By analyzing the literature data, it is clear that relatively small composition variations, within the reduced existence domain of the icosahedral phase in the Al-Pd-Mn system,[28,29] affect strongly the magnetic Mn concentration. However, uncertainties in compositions impede one in determining accurately the link between the composition of the icosahedral phase and the magnetic Mn concentration. For a given composition, the magnetic Mn concentration is modified by thermal treatments[10–12,30] but, under different annealing treatments, the icosahedral F phase can transform into so-called F_2 or F_{2M} structures which are respectively diamond and cubic six-dimensional (6D) superlattices of the icosahedral F phase.[31,32] The respective influences of thermal treatments and structural states on the magnetic properties are not well identified.

Also, the temperature dependence of the magnetic susceptibility is not completely explained. Surprisingly, a Curie law, expected for localized moments without any magnetic

interactions, is not obeyed in the case of samples with a very small concentration of magnetic moments.[13] In the literature, a Curie-Weiss law has often been used to analyze the temperature dependence of the magnetic susceptibility although its validity seems questionable. First of all, the fitted parameters depend on the analyzed temperature range (see, for instance, Ref. 10). Second, the obtained Curie-Weiss temperatures are too large to be explained by magnetic RKKY interactions, at least for the less magnetic samples. In several previous works,[13,25,27] we proposed to explain the temperature dependence of the magnetic susceptibility in Al-Pd-Mn icosahedral phases by a Kondo coupling between localized Mn moment and the conduction electron spins. However, this hypothesis was only tested for a restricted range of magnetic moment concentrations and the possible influence of interactions between magnetic Mn atoms was not examined.

The difficulties encountered in getting an overall understanding of the magnetic properties of icosahedral Al-Pd-Mn phases come from the fact that, in most previous studies, only one or a very few samples were investigated. Then uncertainties in composition, and sometimes in the structural state (F, F_2, or F_{2M}), as well as difficulties in analyzing the temperature dependence of the susceptibility, make comparisons between magnetic data of the literature rather unsatisfactory. In the present work we have undertaken a systematic study of the magnetic properties of icosahedral Al-Pd-Mn phases by studying a large set of samples. They include single crystals and polycrystalline ribbons. Their icosahedral structure is either F, F_2, or F_{2M}. By changing compositions and by applying different thermal treatments, we could span a wide range of variation of the magnetic moment concentration, by a factor around 55. The compositions, thermal treatments, and structures of the studied samples are described in Sec. II and their magnetic properties are presented in Sec. III. By comparing susceptibility data for all studied samples, as well as the literature data, we could demonstrate that the temperature dependence of the susceptibility exhibits a universal behavior whatever the structural state, composition, and thermal treatment of the samples (Sec. IV). This behavior can be explained by a Kondo effect competing with RKKY interactions (Sec. V). This analysis allows us to determine accurately the relative variations of the magnetic moment concentration from sample to sample and to discuss the influence of composition and thermal treatments on magnetic properties (Sec. VI).

II. SAMPLES: THERMAL TREATMENTS, COMPOSITIONS, AND STRUCTURES

We studied pieces cut in large single grains as well as ribbons[1,33] made by rapid quenching from the melt. The origin, composition, annealing treatment, and structural state of each studied sample are given in Table I. Here ''sample'' is used to denote a piece of quasicrystal after a given thermal treatment. For instance samples such as B-a_1 and B-a_2 correspond to the same piece B-a cut in the single grain B, after successive annealing treatments (1) and (2), respectively.

The single grains were grown by the Czochralski technique (described, for instance, in Ref. 34) except single-grain D grown by the Bridgman technique.[28] All the pieces (bars or disks, thickness smaller than 1 mm, weight 0.02–0.2 g) were cut perpendicularly to the growth axis of the single grains. In the case of single-grain B, several pieces were cut at various distances d from the initial seed (37, 33, 32, 6, and 3 mm, respectively, for samples B-a–B-e). Pieces F-a and F-b were cut, respectively, at the bottom (end of growth) and at the top (beginning of growth) of single-grain F.

Within the accuracy of x-ray diffraction, any secondary phases were not detected in the studied samples. However, a very few small precipitates of approximant phases were observed on polished sections by scanning electron microscopy. Because approximant phases in the Al-Pd-Mn system are either nonmagnetic or, at least, only weakly magnetic,[26] such a small quantity of precipitates cannot influence the observed magnetic properties. Besides, a ferromagnetic impurity phase, mostly located at the sample surface, was detected in all samples through magnetization measurements (see Appendix A).

All thermal treatments have been performed under high vacuum (10^{-7} hPa) in alumina crucibles. The procedure called slow cooling (SC) in Table I consists in a heating at 800 °C for 2 h followed by a cooling to either 600 or 500 °C at a rate of 10 °C per hour. This type of thermal treatment is expected to favor structural transformations into F_2 or F_{2M} states for adequate compositions. As neither the composition range nor the kinetics of these structural transitions is accurately known, we have applied the same slow cooling procedure in all cases. In the procedure called rapid cooling (RC), the QC pieces (or ribbons) were heated at 800 °C for 2 h and subsequently cooled to 600 °C within less than 2 min by removing the furnace. This fast cooling procedure should impede structural transformations. Let us note that, prior to the thermal treatments described in Table I, the pieces extracted from single crystals A, B, and C were first annealed at 800 °C for 72 h.

Because of a noncongruent melting, both the liquid and solid compositions change during solidification, resulting in a composition gradient along the single-crystal growth direction. Therefore, it is necessary to analyze the composition of each sample used for magnetic measurements. In the present work, most compositions were determined by x-ray wavelength-dispersive spectroscopy (XWDS) on polished sample faces. The XWDS analyses were calibrated using the atomic composition of sample E-a determined by inductively coupled plasma optical emission spectroscopy (ICP-OES). The error bars for this ICP measurement were Al, 69.4 ± 0.4 at. %; Pd, 21.95 ± 0.3 at. %; and Mn, 8.65 ± 0.1 at. %. The statistic error bars reached in the case of XWDS were in a range of ± 0.05 at. %—i.e., much less than the errors of ICP measurements. Therefore the accuracy on composition variations is better than the accuracy on absolute compositions. Additional ICP-OES analyses were performed on sample B-e and on pieces cut in the immediate neighborhood of samples B-a and F-a (see Table I). The compositions determined by ICP and XWDS for samples B-a and F-a are found compatible within the error bars. In the case of ribbons, the nominal compositions are given in Table I as well as those determined by XWDS.

TABLE I. Samples studied. The different types of structures, determined by transmission electron microscopy, are classified according to Fig. 1: F, $F+\mathrm{diff}\ A3$, F_2, and F_{2M} correspond, respectively, to diffraction patterns (b)–(e). Compositions in bold and italics were measured by XWDS and ICP-OES, respectively. The nominal composition of ribbons is given within parenthesis. Details on the so-called slow cooling (SC) and rapid cooling (RC) procedures are given in the text. The scaling factor α, arbitrarily set equal to 1 for sample *B-b*, is proportional to the atomic concentration of magnetic Mn atoms.

	Composition and origin	Thermal treatment	Structure	α
	Single-crystal *A* [a]			
A-a	$\mathbf{Al_{69.8}Pd_{21.8}Mn_{8.4}}$	2 h 800°C+RC+33h 500°C	F_2	1.5
	Single-crystal *B* [a]			
B-a$_1$	$\mathbf{Al_{70.2}Pd_{21.8}Mn_8}/Al_{70.6}Pd_{21.5}Mn_{7.9}$	2 h 800°C+RC	$F+\mathrm{diff}\ A3$	1.5
B-a$_2$	$\mathbf{Al_{70.2}Pd_{21.8}Mn_8}/Al_{70.6}Pd_{21.5}Mn_{7.9}$	*B-a*$_1$+2 h 800°C+SC→500°C	F_{2M}	0.58
B-b	$\mathbf{Al_{70}Pd_{22.5}Mn_{7.5}}$	2 h 800°C+SC→500°C	F_{2M}	1
B-c$_1$	$\mathbf{Al_{70}Pd_{22.45}Mn_{7.55}}$	2 h 800°C+RC	$F+\mathrm{diff}\ A3$	1.79
B-c$_2$	$\mathbf{Al_{70}Pd_{22.45}Mn_{7.55}}$	*B-c*$_1$+2 h 800°C+SC→500°C	F_2/F_{2M}	1.07
B-d	$\mathbf{Al_{70}Pd_{22.1}Mn_{7.9}}$	2 h 800°C+SC→500°C	$F+\mathrm{diff}\ A3$	2
B-e	$Al_{70.3}Pd_{21.5}Mn_{8.2}$	2 h 800°C+RC	$F+\mathrm{diff}\ A3$	2.92
	Single-crystal *C* [a]			
C-a	$\mathbf{Al_{70.1}Pd_{21.4}Mn_{8.5}}$	2 h 800°C+RC	$(F+\mathrm{diff}\ A3)/F_{2M}$	5.43
	Single-crystal *D* [b]			
D-a	$\mathbf{Al_{70.3}Pd_{21.7}Mn_{8.0}}$	as-grown	F_{2M}	1.85
	Single-crystal *E* [c]			
E-a$_1$	$Al_{69.4}Pd_{21.95}Mn_{8.65}$	as-grown	F	31.5
E-a$_2$	$Al_{69.4}Pd_{21.95}Mn_{8.65}$	*E-a*$_1$+172 h 600°C	$F+\mathrm{diff}\ A3$	18.8
	Single-crystal *F* [a]			
F-a	$\mathbf{Al_{69.7}Pd_{22}Mn_{8.3}}/Al_{69.6}Pd_{22}Mn_{8.4}$	as-grown	$F+\mathrm{diff}\ A3$	7.45
F-b	$\mathbf{Al_{69.1}Pd_{22.5}Mn_{8.4}}$	as-grown	F	19.7
	Single-crystal *G* [d]			
G-a	$\mathbf{Al_{69.5}Pd_{22.15}Mn_{8.35}}$	as-grown	F	7.7
	Single-crystal *H* [d]			
H-a	$\mathbf{Al_{69.7}Pd_{21.8}Mn_{8.5}}$	as-grown	F	10.75
	Ribbons *r-A* [e]			
r-A	$\mathbf{Al_{69.7}Pd_{22.0}Mn_{8.3}}(Al_{70.3}Pd_{21.4}Mn_{8.3})$	2 h 800°C+SC→600°C+20 h 600°C	$F+\mathrm{diff}\ A3$	3.62
	Ribbons *r-B* [e]			
r-B	$\mathbf{Al_{70.4}Pd_{21.2}Mn_{8.4}}(Al_{70.5}Pd_{21}Mn_{8.5})$	4 h 800°C+RC	F	5.25
	Ribbons *r-C* [f]			
r-C	$(Al_{70.5}Pd_{22}Mn_{7.5})$	24 h 750°C+RC	F	1.44

[a]Czochralski growth (CECM).
[b]Bridgman growth, sample (10) in Table II from Ref. 28.
[c]Czochralski growth (LTPCM), Ref. 34.
[d]Czochralski growth (IFF, Jülich).
[e]Planar flow casting (CECM), Ref. 33.
[f]Melt spinning (LEPES), Ref. 1.

The sample structure was characterized by transmission electron microscopy (TEM) investigations carried out on fragments, obtained by crushing small pieces of ribbons or single crystals, deposited on copper grids coated with a carbon film. Structural states can be classified into different categories from electron diffraction patterns of icosahedral twofold zone axis (Fig. 1). As a reference scale, all the diffraction patterns shown in this figure contain a twofold (or pseudotwofold) icosahedral axis in a horizontal position, along which two white crosses mark the positions of both the transmitted beam and a 0/2 0/0 0/0 reflection (or an equivalent reflection to this one). The indexing as $h/h'\ k/k'\ l/l'$

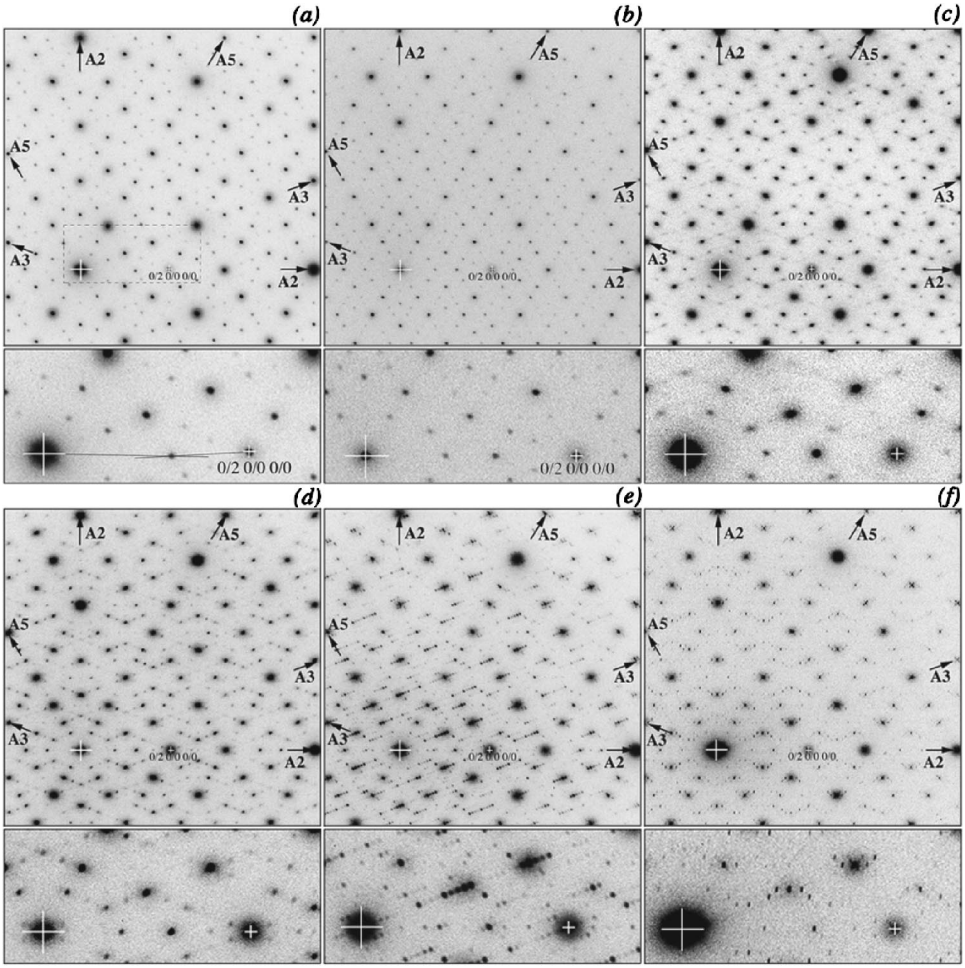

FIG. 1. Electron diffraction patterns of icosahedral or pseudoicosahedral twofold zone axes. The two white crosses mark the positions of both the transmitted beam and a 0/2 0/0 0/0 reflection (or an equivalent reflection to this one). (a) Icosahedral F phase with linear phason strains. (b) Perfect F phase. (c) F phase with weak lines of diffuse scattering parallel to the two threefold axes. (d) F_2 phase. (e) and (f) F_{2M} phase (see text).

$=0/2\ 0/0\ 0/0$ with $Q_{0/2\ 0/0\ 0/0}=1.17\ \text{Å}^{-1}$ was carried out using the scheme proposed by Cahn *et al.*[35] Icosahedral or pseudoicosahedral axes $A5$, $A3$, and $A2$ are indicated on each pattern. Pattern (a) is typical of an icosahedral F phase containing linear phason strains producing jags in reflection rows which are normally aligned for a perfect icosahedral F structure, such as the one observed in pattern (b). The third pattern (c) exhibits icosahedral F reflections together with lines of diffuse scattering parallel to the two threefold axes situated in the plane of the pattern. Note that the intensity of these diffuse scattering lines was found to vary among samples belonging to this group. In pattern (d), additional satellite reflections characteristic of the F_2 structural state[31] are observed. Both the patterns (e) and (f) are related to the F_{2M} phase which has been found to be a stable state resulting of a transformation of the F_2 state.[32] Because of the loss of icosahedral symmetry for five different variants of cubic symmetry, the patterns of F_{2M} along a pseudoicosahedral twofold zone axis [(e) and (f)] are of two types (see Ref. 32). With respect to a vector basis of a 3D cubic system, the zone axis of patterns (e) and (f) correspond to $[\tau^2\ \overline{\tau}\ 1]$ and $[1\ 0\ 0]$, respectively [τ is the golden mean $(1+\sqrt{5})/2$].

The structural state observed by TEM is indicated in Table I for each sample. Several trends have to be emphasized. First, jags in reflection rows were only observed in as-quenched ribbons, not studied here. Second, a well-organized icosahedral F structure, without any measurable diffuse scattering, was found in rapidly cooled ribbons and in several as-grown single crystals, but never in the slowly cooled samples. Third, different heat treatments lead to different structural states in the case of samples B-a and B-c. Finally, in a large single crystal like B, the structural state is not homogeneous: the pieces cut at various distances from the seed exhibit different structural states even after similar thermal treatments. It is clear in Table I for the slow-cooled samples, but it is also true for the rapidly cooled samples ($F+\text{diff}\ A3$) for which the magnitude of the diffuse scattering is not constant. Besides, in some cases, the structural state is even not homogeneous within the sample. For instance, coexisting F_2 and F_{2M} phases were observed within a unique fragment of samples B-c_2 and C-a.

III. MAGNETIC PROPERTIES

Magnetization measurements were performed by an extraction method using a superconductor quantum interference device (SQUID) magnetometer. The magnetization M was measured as a function of temperature in a range of 5–300 K under a fixed magnetic field H (1 and 10 kOe).

The magnetization was also measured at several fixed temperatures as a function of the field (H up to 50 kOe). The magnetic susceptibility of icosahedral Al-Pd-Mn phases be-

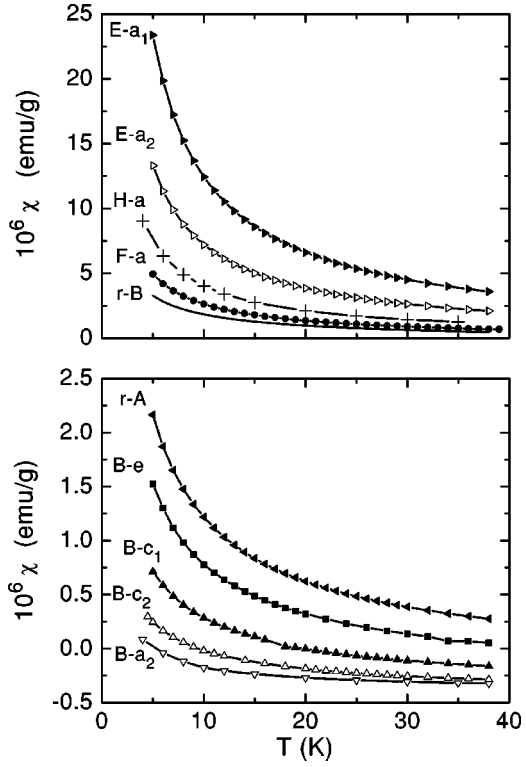

FIG. 2. Temperature dependence of the susceptibility χ, equal to M/H in 1 kOe, corrected from the ferromagnetic contribution as explained in Appendix A. Lines are guides to the eye. Sample labels refer to Table I. The magnitude of the susceptibility varies by a factor 55 between the more magnetic sample E-a_1 and the less magnetic one B-a_2.

ing isotropic,[3] the crystallographic orientation of single crystal samples with respect to the field direction was not determined. Besides, demagnetizing field effects being negligible, any correction due to different sample shapes (disk or bar) was not made.

For all samples, a Curie-like behavior, due to the presence of localized moments, was observed: the magnetization measured in a fixed field was found to decrease with increasing temperature in the range 5–150 K. Besides, a small ferromagneticlike contribution, nearly temperature independent below 150 K, was detected in single crystals as well as in ribbons, by analyzing the field dependence of the measured magnetization at fixed temperatures (see Appendix A). Its magnitude varies from sample to sample. From the results described in Appendix A, it seems reasonable to attribute this ferromagnetic contribution to the presence of a foreign phase, mostly located at the sample surface, which was not detected in structural characterizations. Although the ferromagnetic contribution remains small in all studied samples, it must nevertheless be subtracted from the measured magnetization in order to determine the magnetization of the QC phase. This has been done for all data presented hereafter by using the procedure described in Appendix A.

In the following, we shall focus on the temperature dependence of the magnetic susceptibility χ. Since we observed that the magnetization M of the QC phase varies linearly with the field up to 1 kOe at all temperatures in the range 5–300 K, we could identify χ to M/H for $H=1$ kOe. Typical susceptibility data are shown in Fig. 2. Note that a very large range of susceptibility magnitude, and hence of magnetic moment concentrations, is spanned by the studied samples. From Fig. 2 and Table I, it is clear that small composition changes strongly modify the magnitude of the susceptibility. In addition, for a given piece of single grain, the susceptibility depends on the applied thermal treatment.

Besides, it is striking to observe the existence of an evolution of the susceptibility magnitude along the growth axis of single-grain B: the data obtained for pieces annealed under similar conditions depend on their distance from the seed (see Sec. VI).

For most samples, the susceptibility decreases with in-

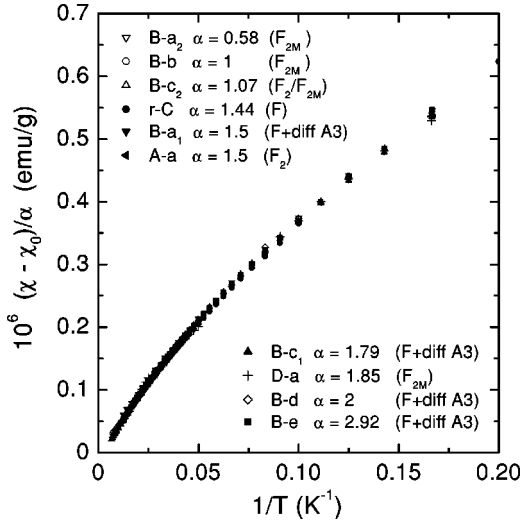

FIG. 3. Scaling of the susceptibility data vs the inverse temperature. χ_0 was estimated by extrapolating the susceptibility in the limit $1/T \rightarrow 0$. The scaling factor α is adjusted so that data for different samples coincide. α has been arbitrarily set equal to 1 for sample B-b. Sample labels refer to Table I.

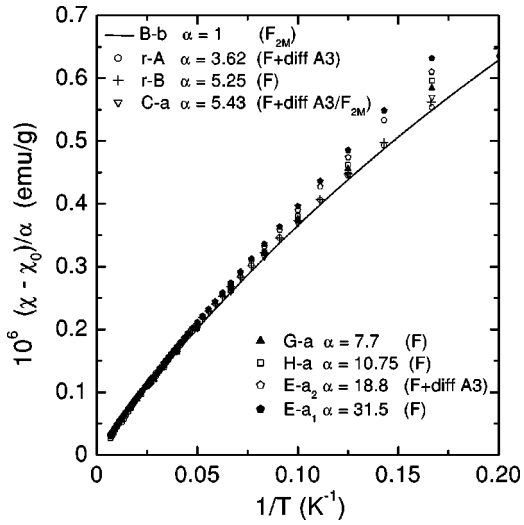

FIG. 4. Same as Fig. 3 but for more magnetic samples.

creasing temperature in the range 5–300 K, but for the less magnetic ones, a slight increase of susceptibility was observed with increasing temperature above 150 K. As shown in Appendix B, such a behavior can be ascribed to a peculiar temperature dependence of the Pauli susceptibility of the conduction electrons in QC phases.[14,36] Below 150 K the Pauli contribution can be considered as temperature independent. Therefore the analysis of susceptibility data was restricted to the range 5–150 K for all samples.

In all cases, we observed that the susceptibility does not vary linearly with the inverse temperature: the $\chi(1/T)$ curves exhibit a continuous curvature (see Fig. 3). Thus, a Curie law ($\chi = C/T$ with C the Curie constant), expected for localized moments without any magnetic interactions, is never obeyed, whatever the magnitude of the susceptibility. These observations are in agreement with previously published results.[1–13] At this step, we shall lay aside the analysis of the temperature dependence of the susceptibility. In the next section, we shall directly compare the susceptibility data measured on different samples and shall establish that Al-Pd-Mn icosahedral phases exhibit a universal magnetic behavior, despite large variations of the susceptibility magnitude from sample to sample.

IV. COMPARISON OF SUSCEPTIBILITY DATA FOR DIFFERENT SAMPLES

We shall first compare the susceptibility data for samples of Table I and then include the literature data.

A. Samples from the present work

Here, we are interested in the contribution of the magnetic Mn atoms to the total susceptibility χ of the QC phase. Thus, we have to subtract a temperature-independent contribution, denoted χ_0, from χ. The χ_0 term accounts for the sum of the Larmor and Pauli contributions. Here, below 150 K, the Pauli contribution can be considered as temperature independent: see Appendix B. As the magnetic Mn atom contribution (χ-χ_0) is expected to vanish in the infinite-temperature limit, the χ_0 value was obtained from the extrapolation towards the limit $1/T=0$ of a polynomial fit of $\chi(1/T)$ performed in the temperature range 5–150 K. The obtained χ_0 values, of the order of -0.4×10^{-6} emu/g, were found to vary only slightly from sample to sample.

Then, for each sample, we have plotted $[\chi(T)$-$\chi_0]/\alpha$ versus $1/T$, where α is a scaling factor, adjusted so that all susceptibility data coincide with those of an arbitrarily chosen reference sample (B-b with $\alpha=1$).[37] The α values are reported in Table I. An excellent superposition of the normalized susceptibility data $(\chi$-$\chi_0)/\alpha$ can be obtained in the range 5–150 K for samples with $0.58 \leqslant \alpha \leqslant 3$ (Fig. 3). Thus, in these α and T ranges, the temperature dependence of the susceptibility obeys a single law whatever the structural state, annealing treatment, and composition. Therefore, for these samples, the atomic concentration of magnetic moments (hereafter noted x) is proportional to the scaling factor α.

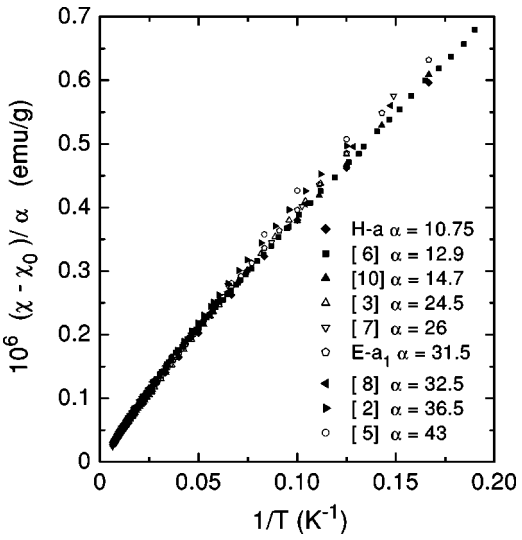

FIG. 5. Scaling of the susceptibility data for literature samples. The corresponding references are given in brackets. The scaling factor α is obtained by setting $\alpha=1$ for sample B-b as in Figs. 3 and 4. Samples H-a and E-a_1 are also drawn for comparison.

For samples with $\alpha \geqslant 3$, scaled susceptibility data can no longer be put into coincidence in the whole temperature range (Fig. 4). In this case, the α values have been determined by superposing susceptibility data from 150 K down to the lowest possible temperature noted T^*. Below T^*, the measured susceptibility is larger than that expected from data obtained for the less magnetic samples. The magnitude of the deviations increases with α. The T^* values increase continuously with α [from 8 K in sample C-a ($\alpha=5.43$) to 20 K in sample E-a ($\alpha=31.5$)]. These low-temperature deviations from the behavior observed in the less magnetic samples can be explained by the presence of magnetic interactions between magnetic Mn atoms, as will be discussed in Sec. V. Anyway at high enough temperature (above T^*) the effect of these magnetic interactions can be neglected and the moment concentration is still proportional to the scaling factor α.

Therefore we can conclude from this scaling procedure that the magnetic moment concentration varies widely, by a factor of about 55, in the samples studied here.

B. Literature samples

Using the same scaling procedure, we analyzed previously published susceptibility data on icosahedral Al-Pd-Mn phases. In most cases, an excellent agreement with the present results was observed: See Fig. 5. There are only a few exceptions which will be examined hereafter. The χ_0 and α values obtained for the literature samples are reported in Table II (with $\alpha=1$ for sample B-b). The α values (from 4.4 to 43) reveal relatively large magnetic Mn concentrations with respect to the less magnetic samples studied in this work. On can note that the χ_0 values reported in Table II are systematically larger than those found for the samples studied in the present work ($\chi_0 \sim -0.4\times10^{-6}$ emu/g). The reason is that no attention has previously been paid to the exis-

TABLE II. Magnetic properties of Al-Pd-Mn icosahedral single crystals from the literature. Structures are indicated when determined by transmission electron microscopy. The scaling factor α is obtained by setting $\alpha=1$ for sample *B-b* as in Table I.

Reference	Thermal treatment	Structure	χ_0 (emu/g)	α
Fisher *et al.* [a]	as-grown	F	$+0.02\times10^{-6}$	12.9
Nimori and Tsai [b]	as-grown		$+0.4\times10^{-6}$	32.5
Matsuo *et al.* [c]	18 h 798°C+quenched	F+diff $A3$	-0.1×10^{-6}	24.5
Saito *et al.* [d]	35 h 806°C+quenched	F	-0.05×10^{-6}	36.5
Escudero *et al.* [e]	as-grown		$+1.4\times10^{-6}$	26
Lasjaunias *et al.* [f]	as-grown		-0.1×10^{-6}	43
Kobayashi *et al.* [g]	sample 1 18 h 802°C, + quenched	F+diff $A3$	-0.15×10^{-6}	14.7
Kobayashi *et al.* [g]	sample 1 20°C→600°C→20°C (steps of 20°C each 20 min)	F_2	-0.32×10^{-6}	4.3

[a]Reference 6.
[b]Reference 8.
[c]Reference 3.
[d]Reference 2.
[e]Reference 7.
[f]Reference 5.
[g]Reference 10.

tence of ferromagnetic contributions. Therefore, the χ_0 values reported in Table II include, in addition to the Pauli and Larmor contributions, a contribution from the ferromagnetic phase (equal to the term noted χ_F in Appendix A). This explains the large dispersion of the χ_0 values and even the occurrence of positive values. We also tried to analyze the susceptibility data of $Al_{71}Pd_{18}Mn_{11}$ ribbons from Ref. 5. However, in this very magnetic sample, RKKY interactions between magnetic Mn atoms are so strong that they lead to a spin-glass transition at a rather large temperature $T_g=3.6$ K. Then the validity of the scaling procedure is questionable and the obtained α value (110 ± 20), affected by large error bars, is only indicative.[38]

In conclusion, the analysis of literature samples confirms that the magnetic susceptibility of Al-Pd-Mn QC phases obeys a universal behavior. Note that good agreement is found for the single crystal of Ref. 8 ($\alpha=32.7$), despite the strange magnetic behavior observed in low field ($H=100$ Oe). Therefore, the low-field anomalies reported in Ref. 8 are probably due to the presence of an extrinsic ferromagnetic contribution, similar to the ones observed in the presently studied samples (Appendix A). Discrepancies in the scaling procedure were only observed for single crystals of Refs. 4 and 9. In the first case, no scaling could be performed whatever the temperature range. In the second one, susceptibility data could be satisfactorily scaled from 120 K to 28 K with $\alpha=75$ and $\chi_0=1.1\times10^{-6}$ emu/g revealing an appreciable ferromagnetic contribution. However, below 28 K, the normalized susceptibility is much smaller than expected from data on samples with comparable or even smaller α values.[17] Such a behavior is clearly anomalous. Therefore, this sample, used in NMR studies,[9,39] could be nonrepresentative of the universal behavior of icosahedral Al-Pd-Mn phases.

C. Universal magnetic behavior of Al-Pd-Mn icosahedral phases

In summary, the scaling of susceptibility data reveals a universal behavior of the temperature dependence of magnetic susceptibility in Al-Pd-Mn QC phases.

Above a sample-dependent temperature T^*, the temperature dependence of the susceptibility is the same in all samples and reveals therefore a single moment behavior. It follows that the scaling factor α is proportional to the concentration x of magnetic moments. Below T^*, the susceptibility departs from this single-moment behavior. The magnitude of the deviations and the T^* value increase continuously when α and hence the moment concentration increases. For the less magnetic samples, the fact that the scaling is obeyed down to 5 K probably means that T^* is lower than 5 K.

The temperature dependence of the susceptibility exhibits the same behavior in ribbons and in single crystals of different origins, elaborated by different growth techniques (Czochralski, Bridgman, or ''self-flux'' technique in the case of Ref. 6). It is independent of the structural state (F with or without diffuse scattering, F_2, or F_{2M}). Only α and thus the moment concentration x vary from sample to sample by a factor close to 80 if one considers both the presently studied samples (Table I) and the literature samples (Table II). Therefore this scaling procedure allows a determination of relative variations of the moment concentration between samples, independently of the analysis of the temperature dependence of the susceptibility. Of course a determination of the value of the moment concentration requires such an analysis (see next section).

Finally, once the contribution from the ferromagnetic phase has been carefully subtracted (according to the procedure explained in Appendix A), the temperature-independent contribution χ_0, due to the sum of the positive Pauli and negative Larmor contributions, is found of the order of -0.4×10^{-6} emu/g. This value is similar to the susceptibilities measured for Al-Cu-Fe and Al-Pd-Re quasicrystals with no localized moments.[14,16] Thus, the large negative values for χ_0 in icosahedral Al-Pd-Mn QC phases are in a favor of a small Pauli contribution and hence of a reduced total density of states at the Fermi level, in agreement with results of specific heat measurements.[4,5]

V. ANALYSIS OF THE TEMPERATURE DEPENDENCE OF THE MAGNETIC SUSCEPTIBILITY WITHIN A KONDO MODEL

The curvature of the $\chi(1/T)$ curves (Figs. 3 and 4) is more pronounced for samples with small α values and, hence, small moment concentrations. This observation discards an origin of these curvatures due to magnetic interactions between the magnetic Mn atoms, which would instead increase with x. We shall show that the temperature dependence of the magnetic susceptibility in Al-Pd-Mn icosahedral phases can be explained by a Kondo effect which is due to a coupling between a magnetic moment and the spins of the conduction electrons. We proposed this hypothesis in previous works[13,25,27] but it was only tested for a quite restricted range of magnetism variations.

A. Kondo analysis for a single moment

Let us recall that a Kondo effect is usually encountered in alloys containing $3d$ impurities diluted in a host metallic matrix, such as CuMn or CuFe alloys, as well as in Ce-based heavy-fermion compounds.[40] In the presence of a Kondo coupling ($J\vec{S}\cdot\vec{s}$, with $J<0$), the conduction-electron spins $\vec{s}$ tend to screen the localized spin $\vec{S}$. This screening is only complete at temperatures much lower than a characteristic Kondo temperature T_K ($T_K \propto \exp[-1/|J|\ N(E_F)]$ with $N(E_F)$ the density of states at the Fermi level). It results in a saturation of the susceptibility for $T \ll T_K$ in contrast with the paramagnetic case where χ diverges as $1/T$. For $T \to 0$, the Kondo normalized magnetic susceptibility per magnetic atom $\chi T_K/C$ tends towards a constant universal value.[40] Here, C is the Curie constant: $C = Nxg^2\mu_B^2 S(S+1)/3k_B$ where N is the total number of atoms. For $T \gg T_K$ the presence of a Kondo coupling is revealed by logarithmic deviations from a Curie law. In practice, the Curie limit $\chi = C/T$ is never reached experimentally even in systems with T_K as low as a few mK such as dilute CuMn alloys.

Using the analytical results of the n-channel Kondo model for $n=2S$ (with S the spin of the magnetic atom),[40] the theoretical susceptibility can be computed at all temperatures: $\chi T_K = Cf(T/T_K)$. Hereafter the S dependence[40] of $f(T/T_K)$ will be neglected. In usual alloys, the moment concentration x is known and thus there are only two unknown parameters to be obtained from the fit of the measured susceptibility: the value of the spin S deduced from that of C and the Kondo temperature. However, in the case of Al-Pd-Mn QC phases, x is an additional unknown parameter. Thus the estimate of the fitting parameter C [$\propto xS(S+1)$] cannot provide separate values of x and S. In the following, in order to obtain a value of x, we assumed a value of S equal to 5/2 for Mn atoms in the high-temperature limit, neglecting orbital effects.

A very good fit of susceptibility data can be obtained for the less magnetic Al-Pd-Mn icosahedral phases in the temperature range 5–150 K. An example is shown in Fig. 6 for sample *B-b* (with $\alpha=1$) for which the range of measurements has been extended down to 2 K. This fit provides both the value of $T_K = 1.2$ K and that of $x = 6.5\times10^{-5}$. Therefore, the Kondo analysis allows us to establish a correspondence between the α values determined using the scaling procedure of Sec. IV and the magnetic Mn atomic concentration: $x = 6.5\times10^{-5}\alpha$. Note that the small x values obtained for the less magnetic samples justify the application of a Kondo approach which, strictly speaking, is only valid in a single-impurity limit.

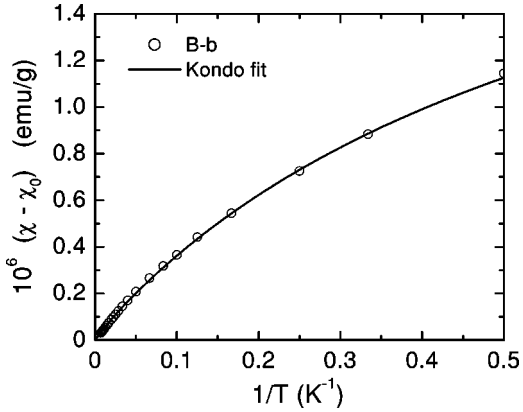

FIG. 6. Fit of the susceptibility data for sample *B-b* in a Kondo model with $T_K = 1.2$ K and a magnetic moment concentration $x = 6.5\times10^{-5}$ (assuming $S=5/2$).

We already mentioned that in many previous works the susceptibility of Al-Pd-Mn QC phases has been fitted by a Curie-Weiss law: $\chi(T) - \chi_0 = C/(T+\Theta)$ where Θ is the Curie-Weiss temperature. Here, let us make three remarks about such fits. First, they were found valid only in restricted temperature ranges so that the values of C, Θ, and χ_0 depend actually on the analyzed T range (see, for instance, Ref. 10). Second, they lead to underestimated values of x. For example in the case of sample *B-b*, a Curie-Weiss fit can be performed in the temperature range 5–80 K. It leads to $\Theta = 2.4$ K and $C = 4.6\times10^{-6}$ emu K/g from which one obtains $x = 4.9\times10^{-5}$ (assuming $S=5/2$) to be compared to $C = 6.2\times10^{-6}$ and thus $x = 6.5\times10^{-5}$ deduced from the Kondo fit. Third, in the literature, the Curie-Weiss temperature Θ was mostly ascribed to magnetic interactions between the localized moments. But, actually, in restricted temperature ranges above T_K, a Curie-Weiss law can describe the theoretical Kondo susceptibility as well.[40] The obtained Θ value is larger than T_K,[40] and the Curie constant is reduced with respect to its high-temperature limit.

B. Competition between Kondo and RKKY interactions

For the less magnetic samples, including sample *B-b*, the success of the scaling down to 5 K shown in Fig. 3 can be interpreted as follows. The susceptibility of these samples follow the same temperature dependence in the range 5–150 K and, consequently, the same Kondo behavior, implying the same Kondo temperature.

Obviously, the susceptibility behavior of more magnetic samples (with $\alpha \geq 3$ and hence $x \geq 2\times10^{-4}$) requires additional explanations. The curvature of the $\chi(1/T)$ curves induced by the Kondo effect still exists but the scaled susceptibility data for these samples do not coincide down to 5 K (see Fig. 4 and Sec. IV A). The low-temperature deviations

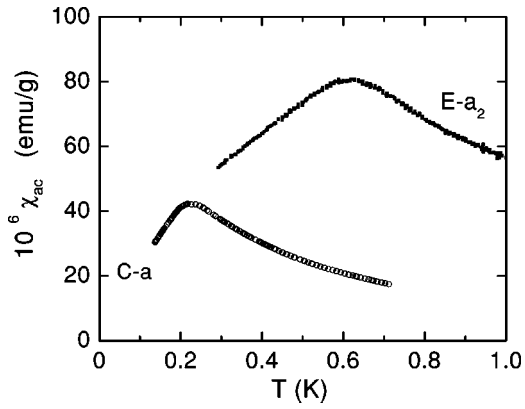

FIG. 7. The ac susceptibility exhibits a cusp at $T_g = 0.23$ K for single-crystal C-a ($x = 3.5\times10^{-4}$) and 0.62 K for single-crystal E-a_2 ($x = 1.2\times10^{-3}$).

from the previous single behavior increase with x. Thus we can assume that they are due to magnetic exchange interactions occurring between magnetic Mn atoms, increasing with x. It is exactly what is expected for a dilute metallic alloy where the magnetic interactions between localized moments are of RKKY type—i.e., mediated by the conduction-electron spins. The energy of the RKKY interaction between two localized moments, separated by a distance r, varies as $1/r^3$. Thus, at a given temperature, the influence of the magnetic interactions increases as the mean distance $\langle r \rangle$ between magnetic Mn atoms decreases—i.e., as x increases. For the less magnetic samples studied here, one cannot exclude the existence of similar low-temperature deviations of $\chi(T)$ from the Kondo susceptibility, due to RKKY interactions, but at temperatures lower than 5 K.

The existence of RKKY interactions in Al-Pd-Mn QC phases is directly revealed by the observation of spin-glass transitions. In the later case, the freezing of the local moments manifests itself by a cusp of the ac susceptibility $\chi_{ac}(T)$ occurring at a temperature T_g. The T_g value is close to the actual transition temperature provided that the magnitude and frequency of the applied ac field remain small enough. We measured the ac susceptibility (frequency, 2 Hz; ac field, 1 Oe) of two samples down to 0.1 K. We used a SQUID magnetometer equipped with a miniature dilution refrigerator. We detected a susceptibility cusp at a temperature $T_g = 0.23$ K for single-crystal C-a ($x = 3.5\times10^{-4}$) and 0.62 K for single-crystal E-a_2 ($x = 1.2\times10^{-3}$): see Fig. 7. These values can be compared with those reported in Ref. 5: $T_g = 1.1$ K for a single crystal to which we ascribed $\alpha = 43$ (and hence $x = 2.8\times10^{-3}$) in Table II and $T_g = 3.6$ K for $Al_{71}Pd_{18}Mn_{11}$ ribbons for which $\alpha = 110\pm20$ (Sec. IV B) and hence $x \sim 7\times10^{-3}$. A T_g value of 0.5 K is reported in Ref. 4 but the susceptibility data for this single crystal could not be satisfactorily scaled (Sec. IV B). If magnetic Mn atoms are randomly diluted, the distance dependence of RKKY interactions ($\propto 1/r^3$) implies that the spin-glass transition temperature T_g increases linearly with x (neglecting any damping effect). The above results are in qualitative agreement with this prediction.

In conclusion, the temperature dependence of the magnetic susceptibility in Al-Pd-Mn QC phases can be explained by a Kondo effect gradually affected by RKKY interactions between magnetic Mn atoms as their concentration increases. Such a competition between Kondo and RKKY couplings is a common behavior in dilute alloys, where the RKKY interactions tend to restore the localized magnetic moment screened by the conduction electrons. For instance $CuMn$ alloys are an example of Kondo systems for Mn concentrations less than 10^{-4} (with T_K of the order of a few mK) and are an archetype of spin glasses for higher Mn contents.[41] In the case of Al-Pd-Mn QC phases, the existence of a Kondo effect is ascertained by measurements of the electrical conductivity $\sigma(T)$ on weakly magnetic samples.[13] Indeed, $\sigma(T)$ was found to increase with decreasing temperature following a $-\ln T$ law. The magnitude of this increase is proportional to the moment concentration. The fact that the conductivity, instead of the resistivity, exhibits these characteristic Kondo features is due to the unconventional transport properties of quasicrystals.[42]

Note that in the previous analysis T_K was assumed to be independent of x and equal to its value in the single-moment limit when magnetic interactions are negligible. The departures from the Kondo fit below T^* have been ascribed to magnetic interactions but the analysis of the susceptibility data has been performed in a restricted temperature range T^*–150 K. Another approach consists in allowing T_K to vary from sample to sample and in analyzing the susceptibility data in a larger temperature range. Such an analysis has been performed in the temperature range 2–150 K in Ref. 13 for weakly magnetic Al-Pd-Mn icosahedral phases. A continuous decrease of T_K has been obtained from 1.2 K to 0.6 K as x increases from 3.7×10^{-5} to 19.3×10^{-5}. In Refs. 25 and 27, a Kondo analysis was applied to single crystals with relatively high magnetic moment concentrations: samples B and C of Ref. 25 are, respectively, samples F-b ($x = 1.28\times10^{-3}$) and F-a ($x = 4.8\times10^{-4}$) of the present work while sample A is close to sample E-a_1 ($x = 2.04\times10^{-3}$). A Kondo fit for these samples in the temperature range 10–300 K leads to $T_K = 0.7$ K. Although these results would suggest that the Kondo temperature is simply renormalized in presence of RKKY interactions and decreases as x increases, the range of analyzed temperatures is too restricted to ascertain this conclusion. Besides, one cannot exclude the existence of an x-dependent distribution of T_K values. Further studies are in progress in order to clarify this point.

Note that the magnetic properties of Al-Pd-Mn icosahedral phases are quite similar to those of metastable Al(Si)-Mn quasicrystals. A Kondo analysis could also be applied to icosahedral and decagonal Al-Mn phases and to the μ-Al_4Mn approximant phase, leading to a slightly larger Kondo temperature of 5.3 K.[27] Also, spin-glass transitions have been observed in metastable Al(Si)Mn phases.[20,43]

VI. DISCUSSION

Although the concentration of magnetic moments in icosahedral Al-Pd-Mn ribbons and single crystals varies widely from sample to sample, it remains small in all cases.

It ranges from $x=3.8\times10^{-5}$ for the less magnetic sample ever studied (sample B-a_2 of the present work) to $x=2.8\times10^{-3}$ for the single crystal of Ref. 5. Therefore only a small fraction of the total number of Mn atoms is magnetic: 4.8×10^{-4} in sample B-a_2 (i.e., one Mn atom over 2000) and 3×10^{-2} in the single crystal of Ref. 5.

Several features indicate that the magnetic moments are well diluted in the quasicrystalline phase. First, the susceptibility can be analyzed in terms of the Kondo effect, which is a single magnetic impurity model. Second, when the RKKY interactions compete with the Kondo effect, one observes a well-defined spin-glass transition, characteristic of a random spatial distribution of the magnetic moments in diluted alloys. Third, it has been shown that the electrical conductivity of weakly magnetic samples varies linearly with the concentration of moments,[13] which therefore act as isolated static defects.

By comparison with approximants and from theoretical considerations on moment formation,[22–24] one can propose that magnetic Mn atoms are associated with particular environments. However, our present understanding of the QC structure[44] is not complete enough to identify such a small number of these particular atomic sites. Meanwhile, one can try to determine parameters governing moment formation.

First, in agreement with previously reported results,[10–12] annealing treatments are found to affect the magnitude of the susceptibility. After a rapid cooling from 800 °C, the concentration of magnetic Mn atoms is systematically found larger than after a slow cooling. The ratio of magnetic Mn concentrations between rapidly and slowly cooled states is 2.6 for sample B-a and 1.7 for sample B-c, to be compared to 3.3 for sample 1 of Ref. 10 (Table II).

Second, magnetic properties are extremely sensitive to composition. It must be emphasized that large variations of the magnetic moment concentration occur for relatively small changes in the quasicrystal composition (Mn, 7.5–8.65 at. %, and Pd, 21.4–22.5 at. %, for the samples in Table I). Note that the largest concentrations of magnetic moments are found in Mn-rich samples. In Ref. 19, an increase of x with the Mn content has been reported in ribbons with high Mn content (from 10 to 15 at. %) which must correspond to metastable QC phases as their compositions are clearly outside the existence domain of icosahedral phases in the Al-Pd-Mn system.[28,29] But it is clear from Table I that the Pd content also influences x. Unfortunately, despite the large number of studied samples, it turned out to be difficult to better characterize the composition dependence of x. Due to the sensitivity of magnetism to thermal treatments, only samples annealed in the same conditions can be compared. As a consequence, as-grown single crystals must be excluded as they were submitted during their growth to uncontrolled thermal treatments.

The extreme sensitivity of the susceptibility magnitude to composition manifests itself by its evolution along the growth axis of single-grain B grown by Czochralski technique (Fig. 8 and Table I). A continuous decrease of the scaling factor and hence of x is observed, both for rapidly and slowly cooled states, as the distance d between the sample and the seed increases. In contrast, no appreciable

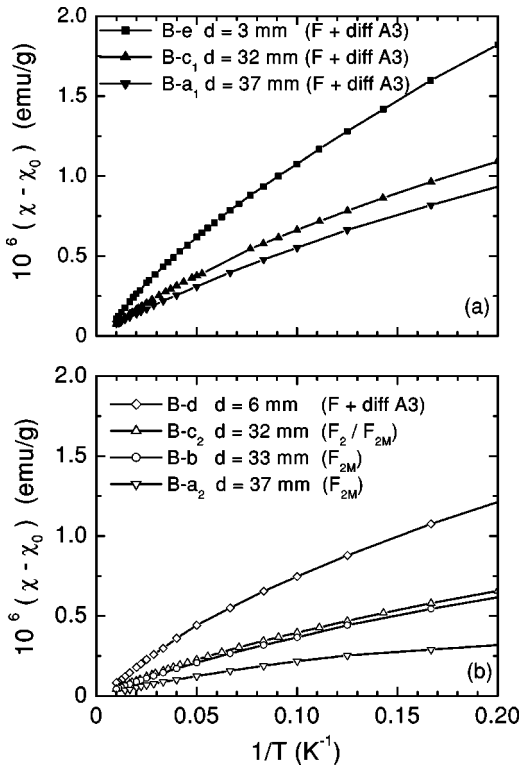

FIG. 8. Susceptibility data for samples cut at different distances d from the seed within single-grain B: (a) rapidly cooled samples, (b) slowly cooled samples. Lines are guides to the eye. Sample labels refer to Table I.

difference was observed between samples B-b and B-c_2 cut at the same distance ($d=30$ mm) on opposite sides of the ingot (10 mm diameter). Let us note that even the small samples used for magnetic measurements are not necessarily homogeneous. Indeed, a decrease of the magnetic Mn concentration by a factor 1.08 was observed after polishing the faces of sample B-e (small disk cut perpendicularly to the growth axis), reducing its mass by 16%. Besides, the structural state of the different samples also changes with d (see Table I and Sec. II).

Therefore neither the magnetic moment concentration nor the structural state is constant along the growth axis of large single grains grown by the Czochralski technique. As a consequence, samples used for magnetic studies have to be cut perpendicularly to the growth axis, as actually done in this work. The same remark applies to samples used in transport studies since the concentration of magnetic Mn directly determines the resistivity.[13] A nonuniform magnetic moment concentration probably also explains the variations of the magnetoresistance along the growth axis of an Al-Pd-Mn single grain reported in Ref. 45.

VII. CONCLUSION

From the present study of the magnetic properties of a large set of samples and comparison between our data and previously published ones, we can draw conclusions for several issues of magnetism in the icosahedral Al-Pd-Mn

phases. The fraction of magnetic Mn atoms is always very small, most of the Mn atoms being nonmagnetic, and the moments are diluted in the quasicrystalline structure. This is in agreement with the dependence of the conductivity of weakly magnetic samples with the moment concentration.[13]

We have shown that the occurrence of magnetic moments is affected by thermal treatments and by small composition changes. Thus, it is clear that magnetism changes reveal subtle structural changes, in agreement with theoretical predictions of a moment formation on Mn atoms influenced by the local and medium range environment.[24] Unfortunately going further is difficult as long as no identification of the sites occupied by magnetic Mn can be performed.

Besides, we have shown that, in Al-Pd-Mn icosahedral phases, the temperature dependence of the susceptibility obeys a universal behavior which is independent of the structural state (F with or without diffuse scattering, F_2, or F_{2M}). Polycrystalline ribbons and single crystals, whatever their elaboration technique, exhibit similar properties. Only the number of magnetic Mn varies from sample to sample. The temperature dependence of the susceptibility can be explained by a Kondo effect gradually affected by RKKY magnetic interactions as the concentration of magnetic Mn atoms increases.

ACKNOWLEDGMENTS

We thank J.C. Rouchaud (CECM, Vitry, France) for ICP measurements and N. Valignat (LTPCM, Saint Martin d'Hères, France) for XWDS analyses. Some of the samples used in this work have been supplied by LTPCM (Saint Martin d'Hères, France), Institut für Feskörperforschung (Jülich, Germany), and LEPES (Grenoble, France). Magnetization measurements were partly performed in Laboratoire de Physique des Solides (Orsay, France). We thank C. Paulsen (CRTBT, Grenoble, France) for his help in ac susceptibility measurements.

APPENDIX A: EVIDENCE FOR A FERROMAGNETIC CONTRIBUTION

In the absence of any ferromagnetic contribution and at large enough temperatures, the measured magnetization M_{meas} is expected to be proportional to the field. Thus the curves M_{meas}/H versus T measured in different fixed fields should coincide. (Differences are only expected at low temperatures when the contribution of localized moments is no more proportional to the field.) It is obviously not the case as is illustrated in Fig. 9(a) for ribbons r-A (nominal composition: $Al_{70.3}Pd_{21.4}Mn_{8.3}$, slowly cooled from 800 to 600 °C). This effect is observed in all samples. It suggests the existence of an additional ferromagnetic contribution of large Curie temperature. Such a contribution is revealed by the analysis of the field dependence of the measured magnetization at constant temperature. Although its presence is not obvious from the $M_{meas}(H)$ curves [Fig. 10(a)], it is clearly observed when $M_{meas}(H)-aH$ is plotted versus H, where the constant a is chosen such that $M_{meas}(H)-aH$ is nearly field independent at large fields [Fig. 10(b)]. Then,

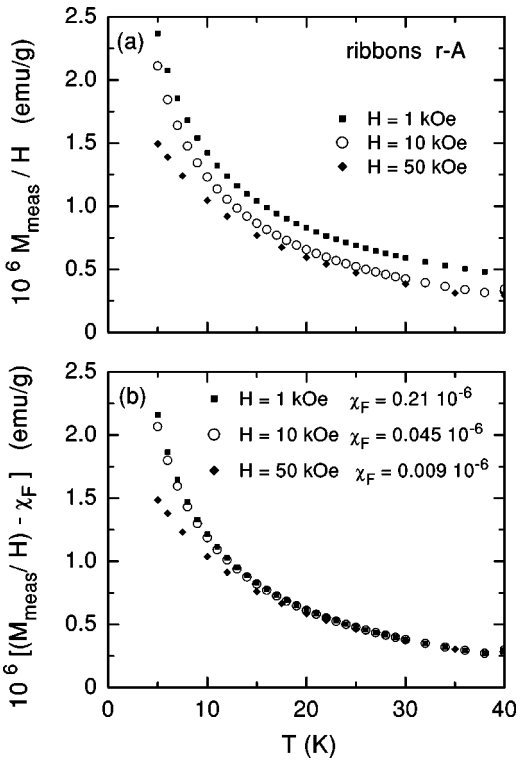

FIG. 9. (a) Temperature dependence of the measured magnetization M_{meas} divided by the applied field H for ribbons r-A (nominal composition $Al_{70.3}Pd_{21.4}Mn_{8.3}$, slowly cooled to 600 °C). (b) Temperature dependence of $M_{meas}/H-\chi_F$, where χ_F is the ferromagnetic contribution determined as explained in the text.

$M_{meas}(H)-aH$ can be identified with the ferromagnetic contribution.

The later reaches saturation above 10 kOe: See Fig. 10(b). The saturated magnetization, denoted M_F, is found nearly temperature independent below 150 K which indicates a Curie temperature above room temperature. The magnitude of M_F varies from sample to sample. For single crystals, M_F is usually of the order of 5×10^{-5} emu/g (for sample mass $\sim$0.2 g). For ribbons, M_F is typically one order of magnitude larger. In a few cases, a marked increase of M_F was observed after an annealing treatment. For single crystals a soft polishing of the surface was then found to reduce appreciably M_F. Therefore, the ferromagnetic contribution could be due to a superficial oxidation of the QC phase. Although its existence has marked consequences on magnetic measurements, due to the very small intrinsic magnetism of the QC phase, it does not affect significantly the composition of the QC phase. For an atomic Mn concentration of 0.08 in the QC phase and a saturated ferromagnetic magnetization $M_F=5\times10^{-5}$ emu per sample gram, the relative fraction of the Mn atoms embedded in the ferromagnetic phase is equal to 10^{-6} (assuming all the Mn atoms in the ferromagnetic phase carry a spin equal to 5/2). In the worse cases, such as for ribbons r-A with $M_F=4.5\times10^{-4}$, this fraction reaches $\sim10^{-5}$.

In order to determine the magnetic contribution of the QC phase as a function of temperature, the contribution of the ferromagnetic phase must be subtracted. As the latter does not depend significantly on temperature below 150 K, one

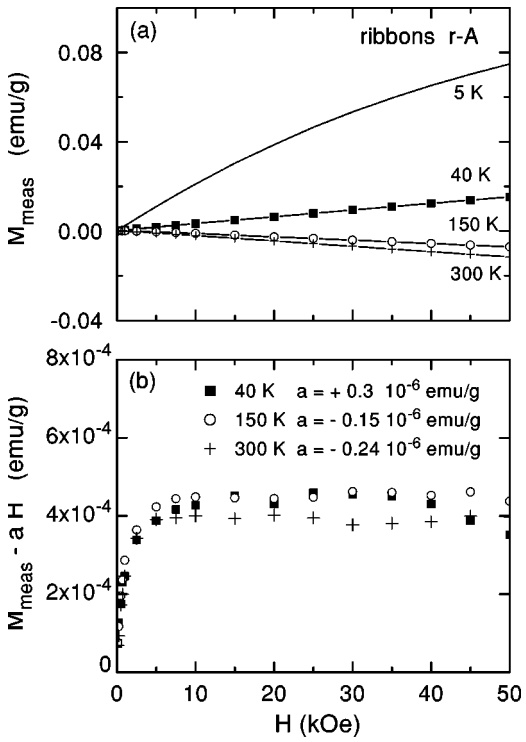

FIG. 10. (a) Measured magnetization vs field at constant temperature for ribbons *r-A* (nominal composition $Al_{70.3}Pd_{21.4}Mn_{8.3}$, slowly cooled to 600 °C). (b) Same data but a term proportional to the field has been subtracted in order to evidence the ferromagnetic contribution.

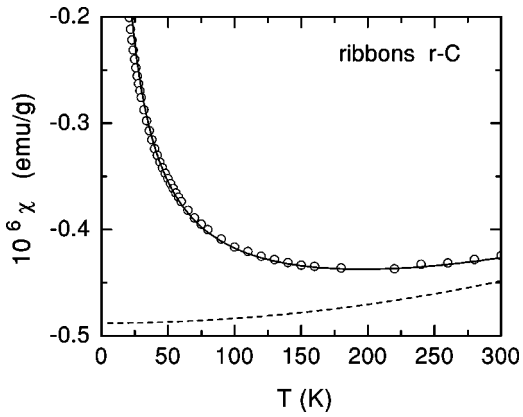

FIG. 11. Temperature dependence of the susceptibility for ribbons *r-C* (nominal composition $Al_{70.5}Pd_{22}Mn_{7.5}$, rapidly cooled from 750 °C). The solid line is a fit to $\chi(T)=\chi_0+C/T+AT^2$ with $\chi_0=-0.488\times10^{-6}$ emu/g, $C=6.6\times10^{-6}$ emu K/g and $A=0.44\times10^{-12}$ emu/(g K^2). The dashed line represents the sum of the χ_0 and AT^2 contributions.

can assume that M/H for the QC phase is equal to $M_{meas}/H-\chi_F$, where χ_F is a field-dependent and temperature-independent constant. In fields larger than 10 kOe, the ferromagnetic contribution being saturated, χ_F is simply equal to M_F/H. Indeed, as shown in Fig. 9(b) for sample *r-A*, for $H=10$ kOe and 50 kOe the $M_{meas}/H-M_F/H$ versus T curves coincide, except of course at low temperature (below 18 K) where the intrinsic magnetization of the QC phase is no more proportional to the field. For $H=1$ kOe, the χ_F value has been determined so that the $M_{meas}/H-\chi_F$ versus T curve coincide with the corrected M/H data in $H=10$ and 50 kOe. The excellent superimposition of all M/H versus T data [Fig. 9(b)] confirms the validity of the previous analysis and the temperature independence of the ferromagnetic contribution at least below 150 K.

The susceptibility data, $\chi=M/H$ for $H=1$ kOe, presented in the core of the present paper have been corrected as explained above. The correction is usually negligible for the more magnetic samples but its relative weight becomes more important for the less magnetic ones. As the ferromagnetic contamination decreases slightly with increasing temperature above 150 K, slight discrepancies are expected, and actually observed for several samples, in the scaling of susceptibility data presented in Sec. IV when data in the range 150–300 K are included. For this reason and also because of the presence of a T^2 contribution in the Pauli susceptibility (see Appendix B), the analysis of susceptibility data was restricted to the range 5–150 K.

APPENDIX B: T^2 CONTRIBUTION TO THE SUSCEPTIBILITY

A small increase of the magnetic susceptibility was detected above 150 K in the less magnetic samples. This can be explained by the existence of a contribution proportional to the square of the temperature. In the range 50–300 K, the susceptibility data of the less magnetic samples studied here can be fitted by assuming $\chi(T)=\chi_0+C/T+AT^2$. For simplification, a Curie law (C/T) was assumed here to describe the contribution of localized moments above 50 K. An example is shown in Fig. 11 for ribbons *r-C* [$A=0.44\times10^{-12}$ emu/(g K^2), $\chi_0=-0.488\times10^{-6}$ emu/g, and $C=6.6\times10^{-6}$ emu K/g].

Such a T^2 contribution had been previously observed in several Al-Pd-Mn icosahedral phases from susceptibility measurements above 300 K.[2,10,18] The magnitude of the T^2 term obtained here is in agreement with the values reported in Refs. 2 and 18. It is slightly higher than the value reported in Ref. 10 because, in addition to the T^2 term, a contribution proportional to T^4 was introduced in Ref. 10. Similar T^2 contributions have also been reported for icosahedral phases with no localized moments in the Al-Cu-Fe and Ga-Mg-Zn systems.[14,36] They have been ascribed to a temperature dependence of the Pauli paramagnetism of conduction electrons caused by a sharp pseudogap in the electronic density of states around the Fermi level.

Although such T^2 contributions are likely present for all the samples studied here, they could be discarded in the analysis of susceptibility data presented in Secs. IV and V. They are obviously completely negligible for the more magnetic samples below 300 K. For the less magnetic ones, such as ribbons *r-C*, their influence is negligible below 150 K. The analysis of susceptibility data was therefore restricted to the range 5–150 K and the Pauli susceptibility was assumed to be temperature independent in this T range.

*Electronic address: Francoise.Hippert@inpg.fr

[1] P. Lanco, T. Klein, C. Berger, F. Cyrot-Lackmann, G. Fourcaudot, and A. Sulpice, Europhys. Lett. **18**, 227 (1992).
[2] K. Saito, S. Matsuo, H. Nakano, T. Ishimasa, and M. Mori, J. Phys. Soc. Jpn. **63**, 1940 (1994).
[3] S. Matsuo, H. Nakano, T. Ishimasa, and M. Mori, J. Phys. Soc. Jpn. **62**, 4044 (1993).
[4] M.A. Chernikov, A. Bernasconi, C. Beeli, A. Schilling, and H.R. Ott, Phys. Rev. B **48**, 3058 (1993).
[5] J.C. Lasjaunias, A. Sulpice, N. Keller, J.J. Préjean, and M. de Boissieu, Phys. Rev. B **52**, 886 (1995).
[6] I.R. Fisher, M.J. Kramer, T.A. Wiener, Z. Islam, A.R. Ross, T.A. Lograsso, A. Kracher, A.I. Goldman, and P.C. Canfield, Philos. Mag. B **79**, 1673 (1999).
[7] R. Escudero, J.C. Lasjaunias, Y. Calvayrac, and M. Boudard, J. Phys.: Condens. Matter **11**, 383 (1999).
[8] S. Nimori and A.P. Tsai, Appl. Phys. Lett. **77**, 280 (2000); J. Magn. Magn. Mater. **241**, 11 (2002).
[9] J. Dolinšek, M. Klanjšek, T. Apih, J.L. Gavilano, K. Giannò, R.H. Ott, J.M. Dubois, and K. Urban, Phys. Rev. B **64**, 024203 (2001).
[10] A. Kobayashi, S. Matsuo, T. Ishimasa, and H. Nakano, J. Phys.: Condens. Matter **9**, 3205 (1997).
[11] S. Matsuo, T. Ishimasa, and H. Nakano, Solid State Commun. **102**, 575 (1997); S. Matsuo, H. Nakano, and T. Ishimasa, in *Proceedings of the 6th International Conference on Quasicrystals, Tokyo, 1997*, edited by S. Takeuchi and T. Fujiwara (World Scientific, Singapore, 1998), p. 467.
[12] M. Scheffer and J.B. Suck, in *Proceedings of the 7th International Conference on Quasicrystals, Stuttgart, 1999*, edited by F. Gähler, P. Kramer, H-R. Trebin, and K. Urban [Mater. Sci. Eng., A **294–296**, 629 (2000)].
[13] J.J. Préjean, C. Berger, A. Sulpice, and Y. Calvayrac, Phys. Rev. B **65**, 140203 (2002).
[14] S. Matsuo, H. Nakano, T. Ishimasa, and Y. Fukano, J. Phys.: Condens. Matter **1**, 6893 (1989).
[15] Y. Yamada *et al.*, Jpn. J. Appl. Phys., Part 1 **38**, 52 (1999).
[16] C.R. Lin, S.T. Lin, C.R. Wang, S.L. Chou, H.E. Horng, J.M. Cheng, Y.D. Yao, and S.C. Lai, J. Phys.: Condens. Matter **9**, 1509 (1997).
[17] V. Simonet, F. Hippert, C. Berger, and Y. Calvayrac, in *Proceedings of the 8th International Conference on Quasicrystals, Bangalore, 2002* [J. Non-Cryst Solids (to be published)].
[18] V. Simonet, F. Hippert, H. Klein, M. Audier, R. Bellissent, H. Fischer, A.P. Murani, and D. Boursier, Phys. Rev. B **58**, 6273 (1998).
[19] K. Fukamichi, in *Physical Properties of Quasicrystals*, edited by Z.M. Stadnik (Springer, Berlin, 1999), p. 295.
[20] J.J. Préjean, J.C. Lasjaunias, A. Sulpice, D. Mayou, and C. Berger in *Proceedings of the 5th International Conference on Quasicrystals, Avignon, 1995*, edited by C. Janot and R. Mosseri (World Scientific, Singapore, 1995), p. 510.
[21] S. Roche and D. Mayou, Phys. Rev. B **60**, 322 (1999).
[22] G. Trambly de Laissardière, D. Mayou, and D. Nguyen Manh, Europhys. Lett. **21**, 25 (1993).
[23] J. Hafner and M. Krajči, Phys. Rev. B **57**, 2849 (1998); M. Krajči and J. Hafner, *ibid.* **58**, 14 110 (1998); M. Krajči, M. Windisch, J. Hafner, G. Kresse, and M. Mihalkovič, *ibid.* **51**, 17 355 (1995).
[24] G. Trambly de Laissardière and D. Mayou, Phys. Rev. Lett. **85**, 3273 (2000).
[25] V. Simonet, F. Hippert, M. Audier, and G. Trambly de Laissardière, Phys. Rev. B **58**, 8865 (1998).
[26] F. Hippert, V. Simonet, G. Trambly de Laissardière, M. Audier, and Y. Calvayrac, J. Phys.: Condens. Matter **11**, 10 419 (1999).
[27] F. Hippert, V. Simonet, M. Audier, Y. Calvayrac, R. Bellissent, G. Trambly de Laissardière, and D. Mayou, in *Quasicrystals—Preparation, Properties and Applications*, edited by E. Belin-Ferré, P.A. Thiel, A.P. Tsai, and K. Urban, Mater. Res. Soc. Symp. Proc. No. 643 (Materials Reasearch Society, Pittsburgh, 2001), p. K14.2.
[28] M. Audier, M. Durand-Charre, and M. de Boissieu, Philos. Mag. B **68**, 607 (1993).
[29] T. Gödecke T and R. Lück, Metallkde **86**, 109 (1995); B. Grushko, M. Yurechko, and N. Tamura, J. Alloys Compd. **290**, 164 (1999); B. Grushko, in *Proceedings of the 7th International Conference on Quasicrystals, Stuttgart, 1999*, edited by F. Gähler, P. Kramer, H-R. Trebin, and K. Urban [Mater. Sci. Eng., A **294–296**, 45 (2000)].
[30] M. Scheffer and R. Lück, in *Aperiodics 97*, edited by M. de Boissieu, J-L. Verger-Gaugry, and R. Currat (World Scientific, Singapore, 1998), p. 469.
[31] T. Ishimasa, Philos. Mag. Lett. **71**, 11 (1995).
[32] M. Audier, M. Duneau, M. de Boissieu, M. Boudard, and A. Letoublon, Philos. Mag. A **79**, 255 (1999).
[33] P. Ochin, in *New Horizons in Quasicrystals*, edited by P.A. Thiel and J.M. Dubois (World Scientific, Singapore, 1996), p. 53.
[34] M. Boudard, E. Bourgeat-Lami, M. de Boissieu, C. Janot, M. Durand-Charre, H. Klein, M. Audier, and B. Hennion, Philos. Mag. Lett. **71**, 11 (1995).
[35] J.W. Cahn, D. Shechtman, and D. Gratias, J. Mater. Res. **1**, 13 (1986).
[36] K. Saito, S. Matsuo, and T. Ishimasa, J. Phys. Soc. Jpn. **62**, 604 (1993).
[37] A similar scaling procedure has previously been used in Refs. 25 and 27 where it was applied to a much more reduced range of magnetism variation. The scaling factor used in these preliminary works was proportional to the inverse of the magnetic moment concentration.
[38] Ribbons studied in Ref. 19, with T_g values larger than 7 K, have not been considered here since a scaling of their susceptibility data would not have been meaningful.
[39] J.L. Gavilano, D. Rau, Sh. Mushkolaj, H.R. Ott, J. Dolinšek, and K. Urban, Phys. Rev. B **65**, 214202 (2002).
[40] A.C. Hewson, *The Kondo Problem to Heavy Fermions* (Cambridge University Press, Cambridge, England, 1993); P. Schlottmann and P.D. Sacramento, Adv. Phys. **42**, 641 (1993).
[41] R. Omari, J.J. Préjean, and J. Souletie, J. Phys. (Paris) **44**, 1069 (1983).
[42] D. Mayou, C. Berger, F. Cyrot-Lakmann, T. Klein, and P. Lanco, Phys. Rev. Lett. **70**, 3915 (1993).
[43] C. Berger and J.J. Préjean, Phys. Rev. Lett. **64**, 1769 (1990).
[44] M. Boudard, M. de Boissieu, C. Janot, G. Heger, C. Beeli, H.U. Nissen, P. Vincent, R. Ibberson, M. Audier, and J.M. Dubois, J. Phys.: Condens. Matter **4**, 10 149 (1992); D. Gratias, F. Puyraimond, M. Quiquandon, and A. Katz, Phys. Rev. B **63**, 024202 (2001).
[45] M. Rodmar, B. Grushko, N. Tamura, K. Urban, and O. Rapp, Phys. Rev. B **60**, 7208 (1999).